Enabling Uncoordinated Dynamic Spectrum Sharing Between LTE and NR Networks

Merkebu Girmay, Vasilis Maglogiannis, Dries Naudts, Timo De Waele, Eli De Poorter, Adnan Shahid, *Senior Member, IEEE*, H. Vincent Poor, *Life Fellow, IEEE*, and Ingrid Moerman, *Senior Member, IEEE*

***Abstract*—Dynamic Spectrum Sharing (DSS) is an enabler for a seamless transition from 4G Long Term Evolution (LTE) to 5G New Radio (NR) by utilizing existing LTE bands without static spectrum re-farming. In this paper, we propose a cross-band DSS scheme that utilizes the Multimedia Broadcast Multicast Service over a Single Frequency Network (MBSFN) feature of an LTE network and the Multicast Broadcast Service (MBS) feature of an NR network. The proposed DSS scheme utilizes LTE and NR resource controllers to assign muted MBSFN subframes on the LTE band and muted MBS subframes on the NR band based on traffic needs. In contrast to the state-of-the-art, the proposed DSS scheme does not require a coordination signaling channel between the LTE and NR networks. Instead, a machine learning-based Technology Recognition and Traffic Characterization (TRTC) system is used to identify and characterize traffic patterns. The LTE and NR resource controllers use the TRTC to sense the muted subframes and offload traffic accordingly. On average, the proposed DSS, as compared to static band configuration, improves the LTE throughput, NR throughput, LTE band spectrum utilization efficiency, and NR band spectrum utilization efficiency by 13.5%, 8.3%, 11.8%, and 20.7%, respectively.**

***Index Terms*—Spectrum sharing, DSS, 4G LTE, 5G NR, Technology recognition, MBSFN, MBS.**

I. Introduction

THE fifth generation (5G) of cellular networks envisions providing 1000 times increased capacity, 10-100 times higher data rates, and supporting 10-100 times more connected devices as compared to the legacy 4G Long-term Evolution (LTE) wireless networks [1]. These high numbers were supposed to be achieved if 5G New Radio (NR) operates in both FR1 (410 MHz – 7125 MHz) and FR2 (24250 MHz – 52600 MHz) 3GPP standard frequency ranges [2]. Even though operating 5G NR on high frequencies with a broader bandwidth may result in faster data rates, using these high bandwidths would be unfavorable in terms of coverage due to the significant signal loss experienced through signal propagation and penetration. In contrast, lower frequency bands (FR1), such as those in the C band or below, provide better coverage and penetration characteristics, making them more suitable for providing wide-area coverage and maintaining connectivity in challenging urban and indoor environments. However, there is an insufficient amount of available frequency resources in the C band to meet the 5G requirements.

In this direction, deploying 5G in the lower frequency bands, which are primarily occupied by 4G frequencies, can provide a significant improvement in spectrum utilization efficiency and capacity. Dynamic Spectrum Sharing (DSS) is a method that enables the utilization of 4G LTE spectrum by 5G NR by implementing the co-existence of the two Radio Access Technologies (RATs) [3].

One of the LTE-NR DSS implementation options in the 3GPP standard is to utilize empty Multi-Broadcast Single-Frequency Network (MBSFN) subframes to enable the coexistence [4]. MBSFN is a feature utilized in Evolved Multimedia Broadcast Multicast Services (eMBMS)-based LTE point-to-multipoint transmissions. Within an LTE MBSFN frame, up to six subframes can be reserved for multicast transmissions, while the rest can be used for unicast traffic. In LTE-NR DSS solutions, this MBSFN feature of LTE is used to share resources between NR and LTE networks. In MBSFN-based DSS, the LTE scheduler schedules its traffic in certain frames, while in the other frames, MBSFN subframes are allocated [4]. In each LTE MBSFN frame, the resources normally assigned for multicast traffic and control information are completely muted so that the duration reserved for these symbols can be used for 5G NR transmission rather than eMBMS. The NR scheduler, on the other hand, schedules its traffic in these muted LTE MBSFN subframes.

In the MBSFN-based DSS, this technique is used to enable the coexistence of LTE and NR traffic in a band primarily configured for an existing LTE network. However, when the traffic load on the 5G network is low, its spectrum may be underutilized. Therefore, this paper proposes a cross-band DSS scheme where both LTE and NR networks can share spectrum in the LTE and NR bands. Throughout this paper, the terms ”LTE band” and ”NR band” refer to the basic bands primarily configured for the LTE and NR networks, respectively.

In the LTE band, the proposed cross-band DSS scheme uses standard muted MBSFN subframe-based DSS. An intelligent LTE resource controller that uses a dynamic resource pool management scheme to adaptively allocate resources to the

This work was supported in part by the European H2020 Program under grant agreement 101016499 (DEDICAT6G project), by the Horizon Europe program under the MCSA Staff Exchanges 2021 grant agreement 101086218 (EVOLVE project), by the Belgian Defense through Contract No. 22DE-FRA004 (DEFRA-BOLSTER project), and by the U.S. National Science Foundation under Grants CNS-2128448 and ECCS-2335876.

M. Girmay, V. Maglogiannis, D. Naudts, T. De Waele, E. De Poorter, A. Shahid, and I. Moerman are with IDLab, Department of Information Technology at Ghent University - imec, Ghent, Belgium (e-mail: merkebutekaw.girmay@ugent.be; vasilis.maglogiannis@ugent.be; dries.naudts@ugent.be; timo.dewaele@ugent.be; eli.depoorter@ugent.be, adnan.shahid@ugent.be; ingrid.moerman@ugent.be).

H. V. Poor is with the Department of Electrical and Computer Engineering at Princeton University, USA (e-mail: poor@princeton.edu).

LTE scheduler is proposed. The LTE resource pool management scheme allocates resources in certain subframes for the LTE scheduler based on the LTE traffic, while the resources in the remaining subframes are muted MBSFN subframes that can be exploited by the NR network.

For the NR band, this work proposes a novel, muted Multicast and Broadcast Services (MBS) subframe-based coexistence scheme. The MBS feature of the 5G NR network released in 3GPP Release 17 [5] can be used to schedule muted NR subframes, giving LTE traffic the opportunity to exploit it. As compared to the MBSFN parameter configuration of LTE [6], the flexibility of the NR physical layer enables a more flexible number of muted NR subframes. In this direction, this paper proposes an advanced NR resource controller that utilizes a dynamic resource pool management scheme to adaptively allocate resources to the NR scheduler. Based on NR traffic, the NR resource controller assigns a selection of subframes to the NR scheduler. The remaining subframes are assigned to be muted MBS subframes and can be utilized by the LTE network.

In the state-of-the-art, the DSS between LTE and NR networks is achieved using a cell resource coordination procedure between the NR gNodeB (gNB) and LTE eNodeB (eNB) over the X2 interface [7]. However, this radio scheduling synchronization leads to additional signaling overhead for DSS between the LTE and NR networks, and it is infeasible for uncoordinated LTE and NR networks. As a solution to this, this work proposes a DSS scheme for uncoordinated LTE-NR networks. The proposed DSS scheme employs Technology Recognition and Traffic Characterization (TRTC) model-based spectrum sensing in both technologies to manage resource scheduling coordination. The NR resource controller uses the TRTC to sense the available spectrum in the LTE band and allocates resources to the NR scheduler accordingly. Similarly, the LTE resource controller uses the TRTC system to sense the available spectrum in the NR band.

In summary, the key contributions of this work are as follows:

- Novel spectrum-efficient resource pool management schemes are proposed for the LTE and NR schedulers. A dynamic LTE resource pool management scheme is introduced to allocate muted MBSFN subframes within the primary LTE band in response to varying LTE traffic loads. Additionally, a novel NR resource pool management scheme is proposed for the dynamic allocation of muted MBS subframes within the primary NR band, considering the NR traffic load. These muted subframes within each band are implemented to enable the use of unused resources by the secondary network.
- To enable LTE-NR DSS without coordination signaling between the technologies, we developed a Convolutional Neural Network (CNN)-based technology recognition model to identify LTE, NR, and overlap signals. Fast Fourier Transform (FFT) of the collected In-phase and Quadrature (IQ) samples is used to train and validate the developed CNN-based technology recognition model.
- A traffic pattern characterization scheme is also proposed to estimate the pattern of the muted LTE MBSFN subframes and muted NR MBS subframes that can be exploited by the NR and LTE schedulers, respectively.
- A cross-band spectrum sharing scheme is proposed to offload LTE traffic to the NR band and vice versa. The resource controllers use the TRTC system to estimate the spectrum unused by the primary network of the band, and these resources are added to the resource pool of the secondary network scheduler.

The rest of this paper is structured as follows: Section II reviews recent studies on LTE-NR coexistence schemes and spectrum sensing mechanisms used in uncoordinated networks. Section III analyzes the challenge addressed in this work and mathematically describes the proposed solution. Section V presents and discusses the performance evaluation of the proposed mechanism. Finally, Section VI presents the conclusion of this work and outlines potential future works.

II. Related Work

Spectrum refarming has emerged as a noteworthy technical strategy for the introduction of 5G networks. Authors in [8] present that when the spectrum of the preceding-generation technology is partitioned and reallocated to the 5G network, there arises an insufficiency in spectrum availability to accommodate traffic from all users. Furthermore, executing spectrum refarming necessitates an effective design strategy aimed at minimizing any disruption to current users. To tackle this problem, 3GPP Release 15 [9] proposed DSS technology as a means to transition from 4G LTE to 5G NR. DSS was subsequently incorporated in Release 16 [10] and further improved in Release 17. Since the standardization, many DSS solutions have been proposed.

In [11], the authors presented two DSS interference mitigation techniques: buffer setting and rate matching. Similarly, in [12], Xin *et al.* demonstrate that dynamic spectrum sharing between 4G and 5G users can lead to substantial interference. They also point out that inter-cell interference, which is caused by cell reference signals from LTE cells, severely impacts the performance of the 5G system. The authors suggest several mechanisms to mitigate interference, including resource element-level rate matching, resource block-level rate matching, and control channel avoidance. To further enhance the 5G system's performance, the authors propose advanced techniques such as multiple Cell-specific Reference Signal (CRS) patterns and cross-carrier scheduling.

In [13], the development and primary implementation methods of the DSS solution are presented. The results of this work indicate that co-frequency interference can have a significant impact on the performance of DSS solutions. Similarly, authors in [14] propose different sharing ratios for resource allocation within a frame. The analysis is done using a common resource sharing controller to compute resource sharing ratios between LTE and NR technologies. The authors propose a resource manager that keeps receiving traffic statistics from LTE and NR stations through a coordination channel.

In [15], a machine learning-based framework is proposed for an LTE-NR DSS solution. The authors propose a controller that can intelligently divide resources between LTE and NR.

The authors of [16] also present a technique that allows operators to provide LTE and NR services utilizing the same band in an interleaved manner. The resources allocated to LTE and NR are managed by a common resource manager. This common resource manager is in charge of figuring out the resource sharing ratio and keeping it up to date based on traffic needs. However, the authors consider a controller that has coordinated LTE and NR schedulers, where the exchange of states and decisions is made through a control channel between the two technologies.

In [17], a DSS scheme that consists of NR and LTE resource allocation algorithms is proposed. The LTE and NR resource allocation algorithms interact with each other and depend on each other. Since the environment of the 4G/5G network system is constantly changing, a dual bargaining game model is used, in which each network agent makes control decisions in coordination with the others. Taking into account the current network system status, the two proposed algorithms operate cooperatively and communicate in real time.

Table I summarizes the state-of-the-art LTE-NR DSS schemes highlighted in this section. Most of the existing LTE-NR DSS solutions propose and analyze a spectrum sharing scheme, assuming that both technologies fully share the same band. However, these DSS schemes require agile and synchronized schedulers that protect the control and synchronization signals in each technology [4], which makes them less feasible for implementation. Hence, this work proposes a cross-band DSS scheme, considering that each technology has its own primary band. On the other hand, the state-of-the-art LTE and NR coexistence schemes in the literature consider coordinated LTE and NR networks that deploy a signaling channel between the two technologies. To the best of our knowledge, existing DSS schemes do not utilize wireless technology identification solutions to enable the coexistence of LTE and NR networks without the need for a coordination channel. This paper proposes a novel TRTC system-based DSS solution for uncoordinated LTE and NR networks.

TABLE I: Related work: DSS schemes.

Reference	Interference mitigation	Adaptive allocation	Cross band sharing	Uncoordinated network
[11]	✓	×	×	×
[12]	✓	×	✓	×
[13]	✓	×	×	×
[14]	×	✓	×	×
[15]	×	✓	×	×
[16]	×	✓	×	×
[17]	×	✓	×	×
Proposed	✓	✓	✓	✓

III. System Design and Problem Formulation

In this section, the resource utilization efficiency and system capacity maximization problems are described considering LTE-NR DSS in the primary LTE band and the primary NR band.

A. Assumptions

The proposed muted MBSFN and muted MBS subframe-based DSS schemes utilize the standard MBSFN and MBS features of LTE and NR networks, respectively. These features are introduced for the down-link multicast traffic in FDD LTE and NR networks. Hence, the DSS solution is proposed for spectrum sharing, considering downlink traffic in FDD LTE and NR networks.

When the muted LTE MBSFN and muted NR MBS subframes are used to enable the LTE-NR DSS, the NR gNB and LTE eNB have to be synchronized on a subframe level. This enables the avoidance of overlapping transmission as the subframe timing of both technologies matches. As the MBSFN subframe pattern repeats periodically until a new configuration is selected, there is no need for synchronization at the frame level, i.e., the starting and ending times of LTE and NR frames do not need to be synchronized. Subframe-level synchronization can be achieved using a satellite-based Pulse Per Second (PPS) time synchronization protocol in the LTE eNB and NR gNB sides [18].

B. LTE-NR DSS on LTE band

In MBSFN-based LTE-NR DSS, the LTE utilizes subframes assigned for unicast traffic, while the MBSFN subframes assigned for multicast traffic and control information are completely muted. Based on the length of the non-MBSFN region configured, the first one or two OFDM symbols of each muted MBSFN subframe are used for LTE PDCCH and CRS, while 5G NR can use the MBSFN region of the subframe. Fig. 1 shows the frame structure of LTE in the MBSFN-based DSS. The figure shows that an LTE frame with muted MBSFN subframes occurs in every M_{ρ}^{lb} frames, where M_{ρ}^{lb} is the MBSFN frame periodicity in the LTE band. Based on the standard, every MBSFN frame can have one to six muted MBSFN subframes, with a possible MBSFN frame periodicity ranging from 1 to 32 [19].

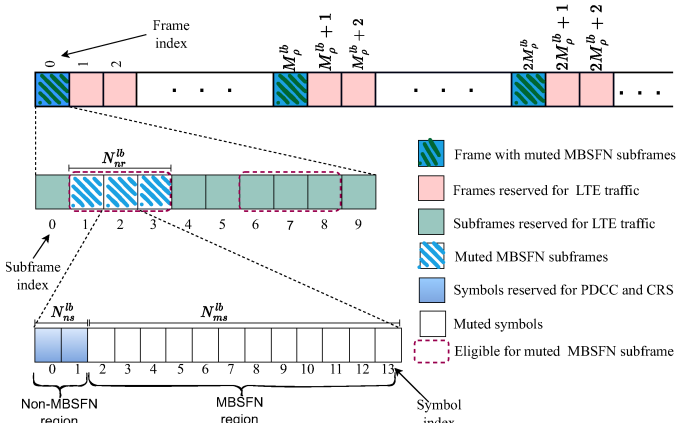

Fig. 1: LTE Frame structure in muted MBSFN subframe based DSS.

In MBSFN-based DSS, each MBSFN frame has N_{nr}^{lb} muted LTE subframes that are available for the NR scheduler, while the subframes assigned to the LTE scheduler (N_{lte}^{lb}) are given as follows:

$$N_{lte}^{lb} = 10 - N_{nr}^{lb}. \quad (1)$$

The LTE capacity is determined by considering the total number of bits scheduled in the subframes available to the LTE scheduler. If an MBSFN configuration $[N_{lte}^{lb}, M_{\rho}^{lb}]$ is used for a window of N_s subframes, the total number of LTE bits scheduled in the window becomes:

$$C_{lte}^{lb}(N_{lte}^{lb}, M_{\rho}^{lb}, N_s) = S_{lte}^{lb}(N_{lte}^{lb}, M_{\rho}^{lb}, N_s) * b_{lte}. \quad (2)$$

Where $S_{lte}^{lb}(N_{lte}^{lb}, M_{\rho}^{lb}, N_s)$ is the number of subframes available for the LTE scheduler (out of the total N_s subframes) and b_{lte} is the total number of bits scheduled in each LTE subframe. The value of b_{lte} depends on the configured bandwidth and the Modulation and Coding Scheme (MCS) [20]. Based on fixed M_{ρ}^{lb} and N_{nr}^{lb}, the number of subframes available for the LTE scheduler becomes:

$$S_{lte}^{lb}(N_{lte}^{lb}, M_{\rho}^{lb}, N_s) = \frac{N_s}{M_{\rho}^{lb}} * \frac{N_{lte}^{lb}}{10} + \frac{(M_{\rho}^{lb} - 1) * N_s}{M_{\rho}^{lb}}. \quad (3)$$

Replacing eq. 3 in eq. 2 and rearranging terms gives:

$$C_{lte}^{lb}(N_{lte}^{lb}, M_{\rho}^{lb}, N_s) = \left(\frac{N_{lte}^{lb}}{10} + M_{\rho}^{lb} - 1\right) \frac{b_{lte} * N_s}{M_{\rho}^{lb}}. \quad (4)$$

Similarly, the NR capacity on the LTE band ($C_{nr}^{lb}(N_{nr}^{lb}, M_{\rho}^{lb}, N_s)$) is computed considering the total number of subframes available for the NR scheduler within the window ($S_{nr}^{lb}(N_{nr}^{lb}, M_{\rho}^{lb}, N_s)$) multiplied by the total number of bits scheduled in each subframe, which is expressed as:

$$C_{nr}^{lb}(N_{nr}^{lb}, M_{\rho}^{lb}, N_s) = S_{nr}^{lb}(N_{nr}^{lb}, M_{\rho}^{lb}, N_s) * b_{nr} * \frac{N_{ms}^{lb}}{N_{ms}^{lb} + N_{ns}^{lb}}. \quad (5)$$

where b_{nr} is the total number of bits scheduled in a subframe. N_{ms}^{lb} and N_{ns}^{lb} represent the number of symbols in the MBSFN region and non-MBSFN region, respectively. The fraction $\frac{N_{ms}^{lb}}{N_{ms}^{lb}+N_{ns}^{lb}}$ is used as the NR traffic can be scheduled in the muted MBSFN region only. Likewise, b_{lte}, the value of b_{nr} corresponding to a specific MCS and bandwidth, is selected based on the 3GPP specification [21].

For a given configuration, the number of subframes available for the NR scheduler (out of the N_s subframes window) becomes:

$$S_{nr}^{lb}(N_{nr}^{lb}, M_{\rho}^{lb}, N_s) = \frac{N_s}{M_{\rho}^{lb}} * \frac{N_{nr}^{lb}}{10}. \quad (6)$$

Replacing eq. 6 in eq. 5 the NR capacity in the LTE band becomes:

$$C_{nr}^{lb}(N_{nr}^{lb}, M_{\rho}^{lb}, N_s) = \frac{N_{nr}^{lb}}{10} * \frac{N_{ms}^{lb}}{N_{ms}^{lb} + N_{ns}^{lb}} * \frac{b_{nr} * N_s}{M_{\rho}^{lb}}. \quad (7)$$

Considering all the resources in the LTE band, the total system capacity becomes:

$$C_s^{lb} = C_{lte}^{lb}(N_{lte}^{lb}, M_{\rho}^{lb}, N_s) + C_{nr}^{lb}(N_{nr}^{lb}, M_{\rho}^{lb}, N_s). \quad (8)$$

The goal here is to propose a scheme that maximizes the total system capacity, C_s^{lb}. Hence, we use the adaptive MBSFN parameter configuration to maximize resource allocation efficiency. In MBSFN-based DSS, the MBSFN parameters can be updated based on the Multicast Channel (MCH) Scheduling Period (S_{ρ}^{lb}). The S_{ρ}^{lb} can take on values ranging from 4 to 1024 ms (in a doubling geometric sequence). Hence, the LTE resource utilization efficiency (ξ_{lte}^{lb}) in an S_{ρ}^{lb} duration can be calculated based on:

$$\xi_{lte}^{lb} = \begin{cases} \frac{Q_{lte}^{lb}}{C_{lte}^{lb}(N_{lte}^{lb}, M_{\rho}^{lb}, S_{\rho}^{lb})} & \text{if } Q_{lte}^{lb} \leq C_{lte}^{lb}(N_{lte}^{lb}, M_{\rho}^{lb}, S_{\rho}^{lb}) \\ 1 & \text{otherwise.} \end{cases} \quad (9)$$

where Q_{lte}^{lb} is the LTE traffic queue length and $C_{lte}^{lb}(N_{lte}^{lb}, M_{\rho}^{lb}, S_{\rho}^{lb})$ is the capacity of resources allocated to LTE within S_{ρ}^{lb} subframes. By considering S_{ρ}^{lb} duration in the LTE capacity equation (eq. 4), $C_{lte}^{lb}(N_{lte}^{lb}, M_{\rho}^{lb}, S_{\rho}^{lb})$ becomes:

$$C_{lte}^{lb}(N_{lte}^{lb}, M_{\rho}^{lb}, S_{\rho}^{lb}) = \left(\frac{N_{lte}^{lb}}{10} + M_{\rho}^{lb} - 1\right) \frac{b_{lte} * S_{\rho}^{lb}}{M_{\rho}^{lb}}. \quad (10)$$

Similarly, the NR resource utilization efficiency (ξ_{nr}^{lb}) in an S_{ρ}^{lb} duration can be calculated based on:

$$\xi_{nr}^{lb} = \begin{cases} \frac{Q_{nr}^{lb}}{C_{nr}^{lb}(N_{nr}^{lb}, M_{\rho}^{lb}, S_{\rho}^{lb})} & \text{if } Q_{nr}^{lb} < C_{nr}^{lb}(N_{nr}^{lb}, M_{\rho}^{lb}, S_{\rho}^{lb}) \\ 1 & \text{otherwise.} \end{cases} \quad (11)$$

where Q_{nr}^{lb} is the NR traffic queue length offloaded to the LTE band and $C_{nr}^{lb}(N_{nr}^{lb}, M_{\rho}^{lb}, S_{\rho}^{lb})$ is the capacity of resources allocated to NR within S_{ρ}^{lb}. Updating the NR Capacity equation (eq. 7) for S_{ρ}^{lb} subframes, $C_{nr}^{lb}(N_{nr}^{lb}, M_{\rho}^{lb}, S_{\rho}^{lb})$ becomes:

$$C_{nr}^{lb}(N_{nr}^{lb}, M_{\rho}^{lb}, S_{\rho}^{lb}) = \frac{S_{\rho}^{lb}}{M_{\rho}^{lb}} * \frac{N_{nr}^{lb}}{10} * \frac{N_{ms}^{lb}}{N_{ms}^{lb} + N_{ns}^{lb}} * b_{nr}. \quad (12)$$

In the muted MBSFN subframe-based DSS, the primary goal is to enhance the LTE resource efficiency by assigning resources based on its traffic demand while leaving the remaining resources for potential NR traffic. Hence, this work proposes an LTE resource allocation scheme that maximizes ξ_{lte}^{lb} keeping the following constraints in consideration:

- In muted MBSFN subframe-based DSS, a single subframe cannot be partially shared for LTE and NR traffic.
- Resources are allocated to LTE traffic based on the possible values of standard MBSFN parameters. As per standard, the number of multicast subframes per MBSFN frame can be $\{1, 2, 3, 4, 5, 6\}$ and periodicity of such frames can be $\{1, 2, 4, 8, 16, 32\}$ frames [19].
- As the LTE UE decodes the LTE SIB2 and SIB13 to determine the MBSFN configuration [19], the resources allocated to LTE can be updated only every 160 ms, which is the minimum possible LTE SIB2 and SIB13 periodicity.
- In the LTE band, the NR scheduler uses resources unused by the LTE scheduler. Hence, the resource allocation on the LTE band considers only the LTE traffic load.

C. LTE-NR DSS on NR Band

In the muted MBS subframe-based LTE-NR DSS, the NR scheduler utilizes subframes assigned for unicast traffic, while subframes assigned for MBS traffic are muted. Unlike MBSFN

in LTE, NR MBS allows a higher degree of flexibility in resource allocation between unicast and multicast traffic [5], [22]. Fig. 2 shows the frame structure of NR in the proposed MBS-based DSS on the NR band. The figure shows that an NR frame with muted MBS subframes occurs in every M_{ρ}^{nb} frame. Based on the standard, NR unicast and NR multicast traffic can be scheduled within resources in a single subframe. However, only subframe-level synchronization is assumed for our proposed LTE-NR DSS. For this reason, we use a configuration that allocates N_{lte}^{nb} muted MBS subframes, where $N_{lte}^{nb} \in \{1, 2, 3, ..., 10\}$ for non-SSB burst frame and $N_{lte}^{nb} \in \{1, 2, 3, 4, 5\}$ for SSB burst frame.

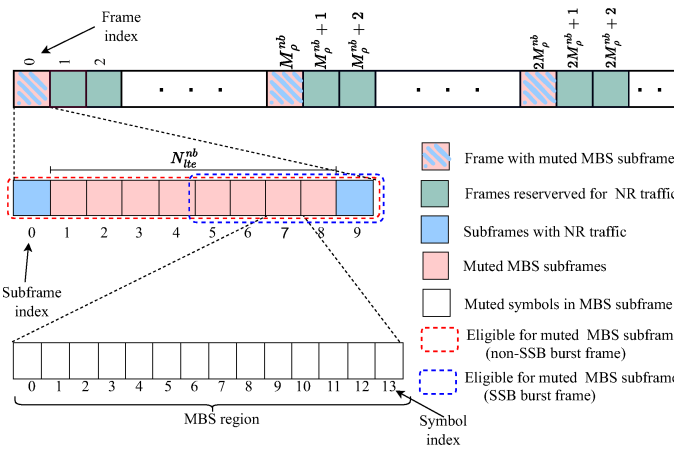

Fig. 2: NR Frame structure in muted MBS subframe-based DSS.

In MBS-based DSS, each MBS frame has N_{lte}^{lb} muted subframes that are available for the LTE scheduler, and the MBS frames are scheduled with a certain MBS frame periodicity (M_{ρ}^{nb}). In the MBS-based DSS in the NR band, subframes assigned for the NR scheduler (N_{nr}^{lb}) are given as:

$$N_{nr}^{nb} = 10 - N_{lte}^{nb}. \tag{13}$$

Using similar procedures used in the LTE-NR DSS on the LTE band, the NR capacity on the NR band ($C_{nr}^{nb}(N_{nr}^{nb}, M_{\rho}^{nb}, N_s)$) based on the configuration $[M_{\rho}^{nb}, N_{nr}^{nb}]$ over the N_s subframes window becomes:

$$C_{nr}^{nb}(N_{nr}^{nb}, M_{\rho}^{nb}, N_s) = \left(\frac{N_{nr}^{nb}}{10} + \frac{M_{\rho}^{nb} - 1}{M_{\rho}^{nb}}\right) \frac{b_{nr} * N_s}{M_{\rho}^{nb}}. \tag{14}$$

where b_{nr} is the total number of bits scheduled in an NR subframe [22].

On the other hand, the LTE uses the muted MBS subframes to offload its traffic, and the LTE capacity in the NR band ($C_{lte}^{nb}(N_{lte}^{nb}, M_{\rho}^{nb}, N_s)$) becomes:

$$C_{lte}^{nb}(N_{lte}^{nb}, M_{\rho}^{nb}, N_s) = \frac{b_{lte}}{M_{\rho}^{nb}} * \frac{N_{lte}^{nb}}{10} * N_s. \tag{15}$$

where b_{lte} is the total number of bits scheduled in an LTE subframe, which is selected based on the MCS and bandwidth [21].

Considering all the resources in the NR band, the total system capacity becomes:

$$C_s^{nb} = C_{nr}^{nb}(N_{nr}^{nb}, M_{\rho}^{nb}, N_s) + C_{lte}^{nb}(N_{lte}^{nb}, M_{\rho}^{nb}, N_s). \tag{16}$$

This total system capacity in the NR band C_s^{nb} is maximized using adaptive MBS parameter configuration that maximizes resource allocation efficiency. In MBS-based DSS, the MBS parameters can be updated based on the traffic queue within the MCH scheduling period (S_{ρ}^{nb}). Hence, the NR resource utilization efficiency in the NR band (ξ_{nr}^{nb}) becomes:

$$\xi_{nr}^{nb} = \begin{cases} \frac{Q_{nr}^{nb}}{C_{nr}^{nb}(N_{nr}^{nb}, M_{\rho}^{nb}, S_{\rho}^{nb})} & \text{if } Q_{nr}^{nb} < C_{nr}^{nb}(N_{nr}^{nb}, M_{\rho}^{nb}, S_{\rho}^{nb}) \\ 1 & \text{otherwise.} \end{cases} \tag{17}$$

where $C_{nr}^{nb}(N_{nr}^{nb}, M_{\rho}^{nb}, S_{\rho}^{nb})$ is the capacity of resources allocated to NR within S_{ρ}^{nb} subframes and Q_{nr}^{nb} is the NR traffic queue length. By considering S_{ρ}^{nb} subframes in the NR capacity equation (eq. 14), $C_{nr}^{nb}(N_{nr}^{nb}, M_{\rho}^{nb}, S_{\rho}^{nb})$ becomes:

$$C_{nr}^{nb}(N_{nr}^{nb}, M_{\rho}^{nb}, S_{\rho}^{nb}) = \left(\frac{N_{nr}^{nb}}{10} + M_{\rho}^{nb} - 1\right) * \frac{b_{nr} * S_{\rho}^{nb}}{M_{\rho}^{nb}}. \tag{18}$$

Similarly, the LTE resource efficiency in the NR band (ξ_{lte}^{nb}) measures how efficiently the LTE scheduler utilizes the muted MBS subframes in an S_{ρ}^{nb} duration, which is given by:

$$\xi_{lte}^{nb} = \begin{cases} \frac{Q_{lte}^{nb}}{C_{lte}^{nb}(N_{lte}^{nb}, M_{\rho}^{nb}, S_{\rho}^{nb})} & \text{if } Q_{lte}^{nb} < C_{lte}^{nb}(N_{lte}^{nb}, M_{\rho}^{nb}, S_{\rho}^{nb}) \\ 1 & \text{otherwise.} \end{cases} \tag{19}$$

where Q_{lte}^{nb} is the LTE traffic queue length offloaded on the NR band and $C_{lte}^{nb}(N_{lte}^{nb}, M_{\rho}^{nb}, S_{\rho}^{nb})$ is the capacity of resources allocated to LTE traffic within S_{ρ}^{nb} period. Updating the LTE Capacity equation (eq. 15) based on the scheduling period S_{ρ}^{nb}, $C_{lte}^{nb}(N_{lte}^{nb}, M_{\rho}^{nb}, S_{\rho}^{nb})$ becomes:

$$C_{lte}^{nb}(N_{lte}^{nb}, M_{\rho}^{nb}, S_{\rho}^{nb}) = \frac{S_{\rho}^{nb}}{M_{\rho}^{nb}} * \frac{N_{lte}^{nb}}{10} * b_{nr}. \tag{20}$$

Generally, the proposed adaptive muted MBS subframe-based DSS aims to maximize resource utilization efficiency while keeping the following constraints into consideration:

- To enable synchronization at the subframe level, a single subframe cannot be partially shared for LTE and NR traffic.
- Muted MBS subframes can be scheduled in every subframe except for subframes in the SSB burst region.
- NR UE decodes SIB20 and SIB21 to determine the MBS configuration used. Hence, the resource allocation update requires at least 80 ms, which is the minimum possible NR SIB20 and SIB21 periodicity [22].
- In the MBS-based DSS on the NR band, the LTE network uses unused resources to offload its traffic, and the resource allocation configuration is made based on NR traffic load only.

IV. Proposed Solution

A. Proposed Resource Coordination in LTE-NR DSS

One basic implementation challenge of DSS is the need for resource allocation synchronization between the LTE eNB and NR gNB [23]. In other words, the NR scheduler must be able to update its resource allocation based on the resources used by the LTE scheduler. Resource coordination between coordinated LTE and NR needs the establishment of a real-time signaling interface. With the help of this coordination channel, the NR scheduler can determine the pattern of the LTE Physical Downlink Shared CHannel (PDSCH) used by the LTE traffic and the always-on LTE Physical Downlink Control CHannel (PDCCH) and CRS, primary synchronization signal, secondary synchronization signal, and Physical Broadcast CHannel (PBCH) of the LTE network. The NR scheduler then schedules its transmission by protecting these LTE signals. On the other hand, the LTE scheduler has to avoid interfering with the NR PDSCH used by the NR traffic, the NR PDCCH, and the NR Synchronization Signal Block (SSB) burst region.

Considering the aforementioned flexibility requirements, the implementation of single-band DSS requires software and hardware modifications on the LTE and NR sides [7]. In order to minimize the need for these additional flexibility features, this work assumes that each technology has its own primary band and that DSS is used to offload user data traffic across the other. This allows each technology to transmit the basic, always-on control signals in its own primary band while providing the flexibility to exploit the unused resources in the other technology's primary band.

The concept of spectrum sharing is expected to be relevant for future networks that aim to utilize dynamic and efficient coverage expansion to ensure quality of service regardless of mobility and location [24]. In such dynamic networks, the cell resource coordination procedure between the NR gNB and LTE eNB over X2 interface synchronization requires complex and dynamic signaling, which makes it less feasible. As a solution, this work proposes a DSS scheme that employs a TRTC system for resource scheduling coordination.

Fig. 3a and Fig. 3b depict the resource coordination methods in DSS mode, illustrating the coordination channel-based approach and the proposed TRTC-based approach, respectively. In the proposed DSS scheme, the NR gNB and LTE eNB use the TRTC system to estimate each other's transmission patterns. For the proposed TRTC-based spectrum sensing, the Radio Unit (RU) is used to capture the IQ samples using its air interface, while the pre-processing and classification can be done on the Distributed Unit (DU) based on the functional split used.

The TRTC system has two parts: (i) technology recognition and (ii) traffic characterization [25]. The technology recognition model is trained and validated to classify three classes: LTE, NR, and overlap of the two signals. The traffic characterization process uses the outcome of the technology recognition model to estimate the traffic pattern. Based on the identified Time Resolution Windows (TRWs), the pattern of the muted LTE MBSFN subframes is determined in the LTE band by the TRTC of the 5G network. Based on the pattern of the muted MBSFN subframes estimated using the TRTC system, the NR resource controller allocates resources (from the LTE band) to the NR scheduler. Similarly, the outcome of the technology recognition process in the LTE network is also used to characterize the pattern of muted MBS NR subframes in the NR band. Based on the estimated pattern of the muted NR MBS subframes, the LTE radio resource controller allocates resources (from the NR band) to the LTE scheduler.

As shown in Fig. 3a, the implementation of resource coordination using a coordination channel in DSS mode demands the exchange of resources among base stations through a dedicated channel. As a result, the execution of this approach poses considerable challenges in terms of compatibility and interoperability, particularly when dealing with base stations operated by various private and public Mobile Network Operators (MNOs). To tackle this problem, our proposed TRTC-based scheme presents a solution that eliminates the need for direct coordination channel communication, thereby mitigating compatibility and interoperability concerns. The proposed TRTC-based resource coordination also enables scalability, as new emerging MNOs do not need to initiate a dedicated coordination channel; rather, the TRTC-based DSS can be used independently.

Another critical challenge in implementing LTE-NR DSS arises from the fact that legacy LTE and NR UE devices are designed to decode the respective LTE and NR reference signals. However, the continuous transmission of these reference symbols leads to significant interference between the LTE and NR technologies, even when only one technology sends traffic at a given time. On the other hand, the alteration of the regular reference symbol pattern necessitates modifications at the UE level, which leads to user experience degradation and increased costs. Implementing such modifications at the UE level often leads to compatibility issues, service disruptions during transitions, and substantial investments in upgrading or replacing devices. As a solution to this, the proposed scheme leverages the MBSFN feature of LTE and the MBS feature of NR to schedule muted MBSFN and muted MBS subframes by the LTE eNB and NR gNB, respectively. This scheduling strategy enables the LTE eNB and NR gNB to signal LTE UEs and NR UEs (respectively) not to anticipate reference symbols during these specific subframes. Our proposed solution thus significantly mitigates interference from reference symbols, all without necessitating modifications in the LTE and NR UEs.

B. Proposed Resource Management Schemes in LTE Band

For the MBSFN-based DSS approach, an efficient resource allocation scheme that adaptively allocates muted MBSFN subframes based on the magnitude of unused resources in the LTE band is proposed. The LTE resource controller uses the proposed resource allocation scheme to determine specific subframes that are required to schedule the traffic based on the LTE traffic load. This leaves the remaining subframes as muted MBSFN subframes that can be used by NR traffic. Resources in the non-muted subframes are added to the LTE scheduler resource pool.

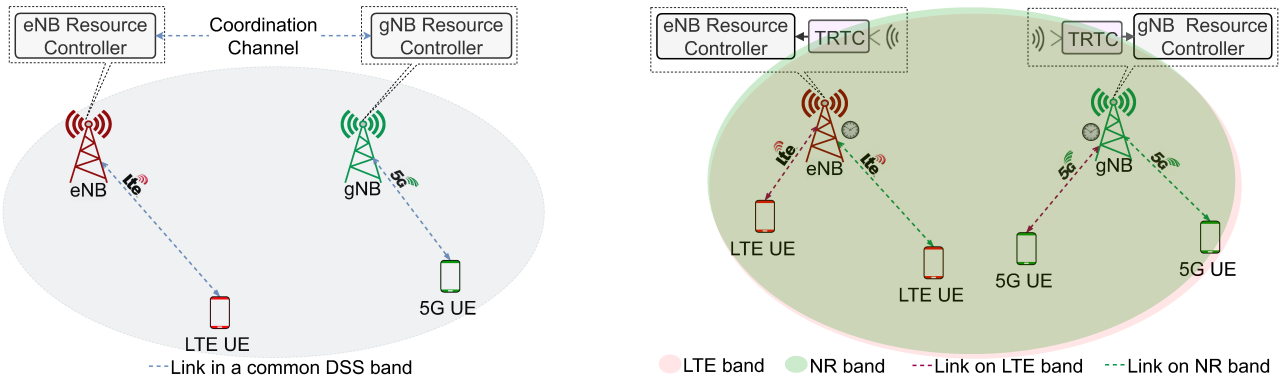

(a) (b)

Fig. 3: Resource coordination in DSS mode a) through coordination channel for coordinated LTE and NR networks b) using proposed TRTC for uncoordinated LTE and NR networks.

According to 3GPP eMBMS specifications [6], the Multicast Coordination Entity (MCE) determines the number of resources required per MCH only when a new service joins or leaves the MBSFN-based MBMS service group. This implies that the resource allocation information in SIB2 and SIB13 is not updated unless a new service joins or leaves the MBMS services group. Similarly, the UE updates the resource allocation provided by a service bearer only when it joins the MBMS service group. In other words, the UE decodes the information in SIB2 and SIB13 when it joins a multicast service and uses the configuration until it leaves the service.

As mentioned before, the number of muted MBSFN subframes in a frame can be fixed to a value between one and six, and the MBSFN period can be varied for increased flexibility. However, fixing the number of muted MBSFN subframes and MBSFN frames to a specific value for the whole multicast service period is not spectrum efficient since the resource allocation will not always be optimal due to the dynamic nature of the traffic. Therefore, it is essential to have a mechanism that adjusts the MBSFN parameter setup for demand-based resource allocation [26].

Algorithm 1: Adaptive resource allocation for LTE scheduler on LTE band.

Input: LTE traffic queue (Q_{lte}^{lb}), eNB frame counter (F_c^{enb})
Output: *Optimal LTE frame configuration in LTE band* (F_{con}^{ltelb})
while true **do**
  // Phase: Compute N_{lte}^{lb} and M_{ρ}^{lb}
  if $F_c^{enb} \,\%\, P_{sib}^{lte} = 0$ **then**
    Update Q_{lte}^{lb}
    $N_{lte}^{lb} \leftarrow \mathrm{V}_{N_{lte}^{lb}}[k]$, $M_{\rho}^{lb} \leftarrow \mathrm{V}_{M_{\rho}^{lb}}[l]$
      // Binary search using eq. 22
  end
  // Phase: Update F_{con}^{ltelb}
  $F_{con}^{ltelb} \leftarrow [\mathrm{N}_{lte}^{lb}, M_{\rho}^{lb}]$
end

Algorithm 1 shows the procedures of the resource allocation scheme used by the LTE resource controller. *Step 4* shows that the resource controller uses the eNB frame index (F_c^{enb}) to periodically check the LTE traffic queue size (Q_{lte}^{lb}) every P_{sib}^{lte} frames. Where P_{sib}^{lte} is the periodicity of the LTE SIB2 and SIB13. Hence, the minimum possible value of P_{sib}^{lte} is 16 frames, which is 160 ms.

Once the size of the traffic queue is determined (in *Step 5*), we use a binary search method in *Step 6* to select the new configuration. For the binary search, a capacity lookup table (C_{table}^{lb}) is generated for each MCS, putting all possible combinations of standard values of N_{lte}^{lb} and M_{ρ}^{lb} in eq. 10. The capacity lookup table is generated by storing and sorting the values obtained using:

$$C_{table}^{lb} = \bigcup_{\forall(i\in I_{lb}, j\in J_{lb})} \{C_{lte}^{lb}(V_{N_{lte}^{lb}}[i], V_{M_{\rho}^{lb}}[j], S_{\rho}^{lb})\}. \quad (21)$$

Where I_{lb} and J_{lb} are sets of the possible indices of $V_{N_{lte}^{lb}}$ and $V_{M_{\rho}^{lb}}$ vectors. $V_{N_{lte}^{lb}}$ and $V_{M_{\rho}^{lb}}$ are vectors that store all the possible values of N_{lte}^{lb} and M_{ρ}^{lb} respectively. According to the 3GPP standard [19] $V_{N_{lte}^{lb}} = \{1, 2, 3, 4, 5, 6\}$ and $V_{M_{\rho}^{lb}} = \{1, 2, 4, 8, 16, 32\}$. At each possible combination $(V_{N_{lte}^{lb}}[I], V_{M_{\rho}^{lb}}[j])$, the $C_{lte}^{lb}(V_{N_{lte}^{lb}}[i], V_{M_{\rho}^{lb}}[j], S_{\rho}^{lb})$ is computed using eq. 10.

The binary search is used to select a target LTE capacity value $(C_{lte}^{lb}(V_{N_{lte}^{lb}}[k], V_{M_{\rho}^{lb}}[l], S_{\rho}^{lb}))$ that corresponds to the new LTE traffic queue size (Q_{lte}^{lb}). The corresponding capacity value is selected from the capacity lookup table in such a way that it satisfies:

$$C_{lte}^{lb}(V_{N_{lte}^{lb}}[k], V_{M_{\rho}^{lb}}[l], S_{\rho}^{lb}) - Q_{lte}^{lb} = \min_{\forall n\in N_{lb}, \delta_{lte}[n]>0} \delta_{lte}[n]. \quad (22)$$

where N_{lb} is a set of possible indices of δ_{lte}. δ_{lte} is a vector that stores the difference between the possible LTE capacity values and the LTE traffic queue size, which is given by:

$$\delta_{lte} = \bigcup_{\forall(i\in I_{lb}, j\in J_{lb})} \{C_{lte}^{lb}(V_{N_{lte}^{lb}}[i], V_{M_{\rho}^{lb}}[j], S_{\rho}^{lb}) - Q_{lte}^{lb}\}. \quad (23)$$

Once the required corresponding capacity value,

$C^{lb}_{lte}(V_{N^{lb}_{lte}}[k], V_{M^{lb}_{\rho}}[l], S^{lb}_{\rho})$ is determined, the values of $V_{N^{lb}_{lte}}[i], V_{M^{lb}_{\rho}}[j]$ that yield this required capacity are used as a new configuration. As shown in *Step 8*, these values are stored in the LTE frame configuration on the LTE band (F^{ltelb}_{con}). Based on the F^{ltelb}_{con}, the resource pool of the LTE scheduler is limited to the resources in the selected non-muted subframes. The newly selected configuration is encoded into the LTE SIBs and sent to the UE.

Algorithm 2: Adaptive resource allocation for NR scheduler on LTE band.

Input: gNB frame counter (F^{gnb}_{c}), gNB subframe index (S^{gnb}_{i})
Output: *Optimal NR frame configuration on LTE band (F^{nrlb}_{con})*
while true **do**
  $F^{nrlb}_{con} \leftarrow$ [N^{lb}_{nr}=0, M^{lb}_{ρ}=0]
  `// Phase: Monitoring I`
  while $N^{lb}_{nr} = 0$ **do**
    for S^{gnb}_{i} = 0 to 9 **do**
      Collect and store IQ samples
    end
    Determine N^{lb}_{nr} using ED
  end
  `// Phase: Monitoring II`
  for F^{gnb}_{c} = 1 to 32 **do**
    for S^{gnb}_{i} = 0 to 9 **do**
      Collect and Store IQ samples
    end
    Determine N^{lb}_{nr} using ED
    if $N^{lb}_{nr} = 0$ **then**
      $M^{lb}_{\rho} \leftarrow M^{lb}_{\rho}$ +1
    else
      $F^{nrlb}_{con} \leftarrow$ [N^{lb}_{nr}, M^{lb}_{ρ}]
      Start running TRTC on gNB
    end
  end
  `// Phase: Main`
  for Every new frame **do**
    Update frame pattern using TRTC
    if Pattern change detected **then**
      Go to Step 4
    else
      $F^{nrlb}_{con} \leftarrow$ [N^{lb}_{nr}, M^{lb}_{ρ}]
    end
  end
end

Algorithm 2 shows the process of the resource allocation algorithm (in the LTE band) for the NR scheduler. *Step 4* shows that the algorithm starts with an initial configuration of $N^{lb}_{nr} = 0$ and $M^{lb}_{\rho} = 0$ stored in the NR frame configuration in the LTE band (F^{nrlb}_{con}). In the *Monitoring I* phase, the NR resource controller initially uses Energy Detection (ED) to determine the number of muted MBSFN subframes (N^{lb}_{nr}) in an LTE frame. For the ED, IQ samples are collected and stored for every subframe (S^{gnb}_{i}) within a frame (*Steps 6–8*). After that, in *Step 9*, the total energy received in every subframe within the frame is compared with a threshold. If the received signal exceeds the threshold, a subframe is identified as a non-muted subframe. Otherwise, it is identified as a muted subframe. This process is repeated for every frame until an LTE frame with N^{lb}_{nr} muted MBSFN subframes is detected, where $N^{lb}_{nr} > 0$. After that, in *Monitoring II* phase, the periodicity of the muted MBSFN subframe pattern (M^{lb}_{ρ}) is determined by using ED for the next consecutive frames. This process takes the gNB frame counter (F^{gnb}_{c}) value to track the frames indexes and it is shown in *Steps 11–22* in the algorithm. Similar to phase *Monitoring I*, the ED-based muted MBSFN subframe pattern determination in a given frame is used (*Steps 12–15*). The value of M^{lb}_{ρ} is determined by counting the frames until a frame with the same number of muted MBSFN subframes is detected. *Steps 16–18* show this counter. This process can take up to 32 frames, which is the maximum standard value of M^{lb}_{ρ}.

In *Step 19* the determined N^{lb}_{nr} and M^{lb}_{ρ} values are stored in the NR frame configuration in the LTE band (F^{nrlb}_{con}). After that, the TRTC system is initiated on the NR gNB. Based on the determined F^{nrlb}_{con}, the NR resource controller determines the resource pool of the NR scheduler. The NR scheduler then starts to schedule the traffic based on the determined NR resource pool (*Main* phase). In this phase, every subframe has the possibility of being unused (free) or occupied by LTE, NR, or overlapping LTE and NR signals, and we cannot use ED to identify the signal types. Hence, in *Step 24* the proposed TRTC process is used to determine the frame pattern. In other words, the TRTC determines the sequence of LTE, NR, and overlap subframes in every new frame. If an unused subframe or a subframe with an overlap signal is detected, it indicates that the number of muted MBSFN subframes assigned by the LTE resource controller has changed. Therefore, the NR resource controller goes back to *Step 4* and triggers a new monitoring process, and the whole process is repeated. Otherwise, the determined resource allocation will be used by the NR scheduler until a change in frame pattern is detected (*Step 28*).

C. Proposed Resource Management Schemes in the NR Band

For the muted MBS subframe-based DSS, a resource scheduling algorithm that adaptively selects MBS parameters based on NR traffic is proposed. The procedures of the resource allocation scheme used by the NR resource controller are presented in Algorithm 3.

Step 5 shows that the NR traffic queue size (Q^{nb}_{nr}) is checked every P^{nr}_{sib} frames. The value of P^{nr}_{sib} is selected based on the NR SIB20 and SIB21 periodicity. The NR resource controller uses the gNB frame index (F^{gnb}_{c}) to periodically check the traffic queue.

Likewise, for the LTE scheduler in the LTE band, a binary search method is used to select the new configuration used by the NR scheduler in the NR band (*Step 6*). When a gNB is activated, a capacity lookup table (C^{nb}_{table}) is generated for each MCS, putting all possible combinations of standard values of

Algorithm 3: Adaptive resource allocation for NR scheduler on NR band.

Input: NR traffic queue (Q_{nr}^{nb}), gNB frame counter (F_c^{gnb})
Output: *Optimal NR frame configuration in NR band* (F_{con}^{nrnb})
while true **do**
  // Phase: Compute N_{nr}^{nb}, M_{ρ}^{nb}
  if $F_c^{gnb} \% P_{sib}^{nr} = 0$ **then**
    Update Q_{nr}^{nb}
    $N_{nr}^{nb} \leftarrow \mathrm{V}_{N_{nr}^{nb}}[k]$, $M_{\rho}^{nb} \leftarrow \mathrm{V}_{M_{\rho}^{nb}}[l]$
      // Binary search using eq. 25
  end
  // Phase: Update F_{con}^{nrnb}
  if $F_c^{gnb} \% P_{ssb} = 0$ **then**
    $N_{nr}^{ssb} \leftarrow \max(N_{nr}^{nb}, 5)$ // SSB frame
    $F_{con}^{nrnb} \leftarrow [\mathrm{N}_{nr}^{ssb}, 1]$
  else
    $F_{con}^{nrnb} \leftarrow [\mathrm{N}_{nr}^{nb}, M_{\rho}^{nb}]$ // Non-SSB frame
  end
end

N_{nr}^{nb} and M_{ρ}^{nb} in eq. 18. The capacity lookup table is generated using:

$$C_{table}^{nb} = \bigcup_{\forall(i \in I_{nb}, j \in J_{nb})} \{C_{nr}^{nb}(V_{N_{nr}^{nb}}[i], V_{M_{\rho}^{nb}}[j], S_{\rho}^{nb})\}. \quad (24)$$

Where $C_{nr}^{nb}(V_{N_{nr}^{nb}}[i], V_{M_{\rho}^{nb}}[j], S_{\rho}^{nb})$ is the capacity computed using eq. 18. $V_{N_{nr}^{nb}}$ and $V_{M_{\rho}^{nb}}$ are vectors that store all the possible values of N_{nr}^{nb} and M_{ρ}^{nb} respectively. I_{nb} and J_{nb} are sets that store all possible indices of $V_{N_{nr}^{nb}}$ and $V_{M_{\rho}^{nb}}$ vectors.

During the execution process, the binary search is used to select a target NR capacity value ($C_{nr}^{nb}(V_{N_{nr}^{nb}}[k], V_{M_{\rho}^{nb}}[l], S_{\rho}^{nb})$) that corresponds to the NR traffic queue size (Q_{nr}^{nb}) is selected from the capacity lookup table in such a way that it satisfies:

$$C_{nr}^{nb}(V_{N_{nr}^{nb}}[k], V_{M_{\rho}^{nb}}[l], S_{\rho}^{nb}) - Q_{nr}^{nb} = \min_{\forall n \in N_{nb}, \delta_{nr}[n] > 0} \delta_{nr}[n]. \quad (25)$$

Where N_{nb} is a set of δ_{nr} indices and δ_{nr} is a vector that stores all the possible difference values between each value stored in the NR capacity lookup table and the NR queue size, which is given by:

$$\delta_{nr} = \bigcup_{\forall(i,j)} \{C_{nr}^{nb}(V_{N_{nr}^{nb}}[i], V_{M_{\rho}^{nb}}[j], S_{\rho}^{nb}) - Q_{nr}^{nb}\}. \quad (26)$$

The values of $V_{N_{nr}^{nb}}[k], V_{M_{\rho}^{nb}}[l]$ that produce the required capacity $C_{nr}^{nb}(V_{N_{nr}^{nb}}[k], V_{M_{\rho}^{nb}}[l], S_{\rho}^{nb})$ are selected as a new NR frame configuration in the NR band (F_{con}^{nrnb}).

The newly selected frame configuration F_{con}^{nrnb} is encoded into the NR SIBs and sent to the UE, and it is used for the next frames until a new configuration is selected based on the traffic queue after a minimum duration of P_{sib}^{nr} frames. However, the selected configuration is used in all frames within the P_{sib}^{nr} window except the NR frames that contain the SSB burst. In 5G NR, the SSB burst region is used for Synchronization Signal (SS) and PBCH. Half of the radio frame window (5 subframes), is the maximum length for an SSB burst, which may contain one or more SS/PBCH blocks. For this reason, *Step 9* shows that at least five subframes are reserved for the NR scheduler in the SSB burst frame. There is some flexibility in the SSB periodicity (P_{ssb}), which can range from 5 to 160 ms [21]. For a frame that contains an SSB burst, the number of NR subframes is set to at least 5, as follows:

$$N_{nr}^{ssb} = \max(N_{nr}^{nb}, 5). \quad (27)$$

where N_{nr}^{ssb} is the number of non-muted subframes in an NR frame that contains the SSB burst.

Step 10 indicates that this frame configuration F_{con}^{nrnb} with N_{nr}^{ssb} non-muted subframes is used for an NR frame with SSB. For the rest frames, the F_{con}^{nrnb} determined by the binary search is used (*Step 12*).

Algorithm 4: Adaptive resource allocation for LTE scheduler on NR band.

Input: eNB frame counter (F_c^{enb}), eNB subframe index (S_i^{enb})
Output: *Optimal LTE frame configuration NR band* (F_{con}^{ltenb})
while true **do**
  $F_{con}^{ltenb} \leftarrow [\mathrm{M}_{\rho}^{nb} = 0, N_{lte}^{nb} = 0]$
  // Step: Monitoring I
  while $N_{lte}^{nb} = 0$ **do**
    for S_i^{enb} = 0 to 9 **do**
      Collect and Store IQ samples
    end
    Determine N_{lte}^{nb} using ED
  end
  // Step: Monitoring II
  for F_c^{enb} = 1 to 32 **do**
    for S_i^{enb} = 0 to 9 **do**
      Collect and Store IQ samples
    end
    Determine N_{lte}^{nb} using ED
    if $N_{lte}^{nb} = 0$ **then**
      $M_{\rho}^{nb} \leftarrow \mathrm{M}_{\rho}^{nb}$ +1
    else
      $F_{con}^{ltenb} \leftarrow [\mathrm{N}_{lte}^{nb}, M_{\rho}^{nb}]$
      Start running TRTC on eNB
    end
  end
  // Step: Main
  for Every new frame **do**
    Update subframe pattern using TRTC
    if Pattern change detected **then**
      Go to Step 4
    else
      $F_{con}^{ltenb} \leftarrow [\mathrm{N}_{lte}^{nb}, M_{\rho}^{nb}]$
    end
  end
end

On the other hand, the LTE resource controller in the eNB senses the pattern of the muted MBS subframes in the NR band and allocates resources to the LTE scheduler accordingly. Algorithm 4 shows the process of the LTE scheduler resource allocation algorithm used by the LTE resource controller on the NR band. *Step 4* shows that the algorithm starts with an initial LTE frame configuration in the NR band (F_{con}^{ltenb}) with values $N_{lte}^{nb} = 0$ and $M_{\rho}^{nb} = 0$.

Subsequently, the process involves utilizing ED to establish the pattern of muted MBS subframes (N_{lte}^{nb}) within NR frames on the NR band. Regarding the ED procedure, IQ samples are gathered and preserved for each subframe (S_i^{enb}) contained within a frame (*Steps 6–8*). Following this, during *Step 9*, the cumulative energy received in each subframe within the frame is compared against a predetermined threshold. If the received signal surpasses the threshold, the subframe is designated as non-muted; otherwise, it is labeled as a muted MBS subframe. This ED process is repeated for every frame until a muted MBS subframe is detected. In other words, this process in *Monitoring I* phase is repeated until $N_{lte}^{nb} \neq 0$.

After that, the repeating pattern periodicity M_{ρ}^{nb} of the frame is found by using ED on subsequent frames (*Monitoring II* phase). The value of M_{ρ}^{nb} is determined by counting the number of frames until a frame with the same number of muted MBS subframes is repeated. This procedure utilizes the eNB frame counter (F_c^{enb}) to monitor frame indices, and the pattern of muted MBS subframes is determined using ED as shown (*Steps 12–15*).

The value of M_{ρ}^{nb} is established by tallying the frames until a frame with an equivalent count of muted MBS subframes is identified, as illustrated in *Steps 16–18*. During *Step 19*, the determined N_{lte}^{nb} and M_{ρ}^{nb} values are stored as the LTE frame configuration for the NR band (F_{con}^{ltenb}). Subsequently, the TRTC system is initiated by the LTE eNB. The LTE resource controller employs the determined F_{con}^{ltenb} to establish the resource pool for the LTE scheduler. The LTE scheduler then commences scheduling traffic based on the designated LTE resource pool (*Main* phase). During this phase, each subframe can either remain unused (idle) or be occupied by LTE, NR, or overlapping LTE and NR signals. In such cases, utilizing ED for signal type identification becomes unfeasible.

Thus, in *Step 24*, the proposed TRTC process is used to determine the frame pattern. The TRTC process determines the sequence of subframes with LTE, NR, and overlapping signal within each frame. The detection of an unused subframe or a subframe containing an overlapping signal indicates a change in the number of muted MBS subframes. Consequently, the NR resource controller returns to *Step 4*, initiating a new monitoring process and repeating the entire cycle. Alternatively, if no change in frame pattern is detected, *Step 28* shows that the determined resource allocation remains in use by the LTE scheduler until a new muted MBS subframe pattern is identified.

V. Results

A. Simulation Parameters

For the performance analysis, the Vienna LTE system-level simulator [27] and the 5G MATLAB Toolbox are used to model the LTE and NR networks, respectively. For the performance evaluation process of the proposed DSS solutions, co-located LTE eNB and NR gNB with omnidirectional antennas are considered. 2680 MHz and 2635 MHz are used as the center frequencies for the primary LTE and NR bands, respectively. 20 MHz bandwidth is used for both bands, and 15 KHz carrier spacing is used for the NR network. Each LTE eNB and NR gNB has N active UEs connected to it at a time, where N is randomly selected using a Poisson distribution between 1 and 100 UEs with a mean of 50 UEs. We also consider that an active UE can join a cell with one of the traffic types with the following probabilities: FTP (10%), HTTP (20%), VoIP (30%), video (20%), and gaming (20%) [28].

Once a UE is connected to a cell, a specific traffic type is selected with these probabilities, and it remains for N_T Transmission Time Intervals (TTIs), where N_T is randomly picked from an interval between 1 and 15. Considering the minimum and maximum values of N_T, it can be observed that the traffic type of each active UE can change 20 to 300 times within the 300 TTI run-time. These values used for simulating dynamic traffic are adopted from [29]. The performance analysis is based on 4,000 runs, where each run has a run time of 300 TTIs.

The periodicities of LTE SIB2/SIB13 and NR SIB20/23 are 160 ms and 80 ms, respectively. Based on these periodicity values, Algorithm 1 and Algorithm 3 are used to determine the resource pool size of the LTE scheduler and NR scheduler, respectively. After determining the available resources, the Proportional Fair (PF) scheduler allocates a given number of resource blocks to each user. In the rest of the paper, the PF LTE scheduler and PF NR scheduler that use the proposed adaptive resource pool size are referred to as the "customized LTE PF scheduler" and "customized NR PF scheduler" for the LTE and NR networks, respectively. For comparison, we also consider a classical PF LTE scheduler and a classical PF NR scheduler that use static LTE and NR bands, respectively.

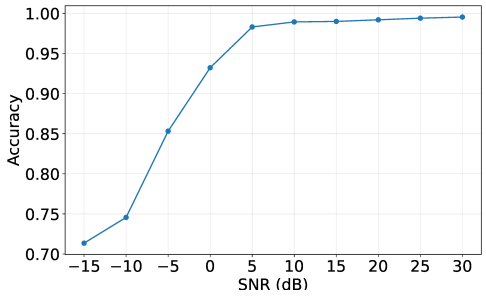

Fig. 4: Classification performance of the proposed CNN model at different SNR levels.

B. Technology Recognition and Traffic Characterization

The CNN architecture comprises three layers, each with a specific purpose. In the first layer, 64 filters of size 1 x 3 capture basic features. The second layer uses 32 filters of size 2 x 3 to capture higher-level features. The third layer, with

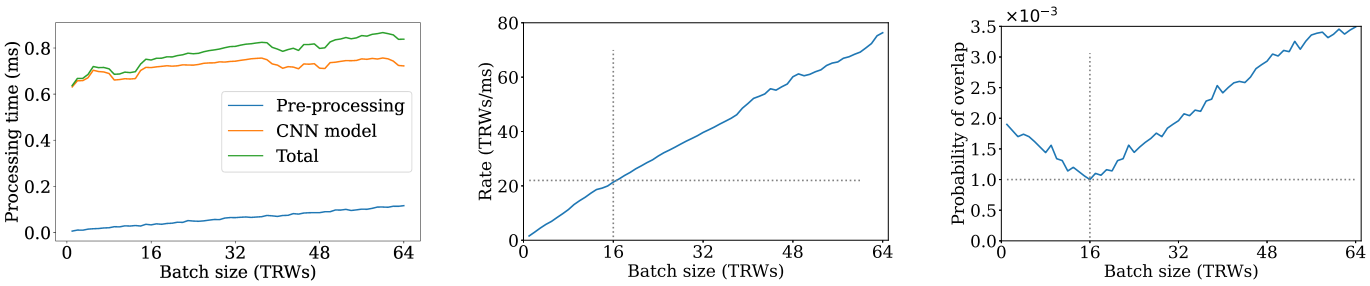

(a) (b) (c)

Fig. 5: Impact of batch size on the TRTC system a) processing time b) classification rate c) probability of overlap TRWs.

16 filters of size 2 x 3, refines feature extraction further. To reduce spatial dimensions, Max-pooling is used between the CNN layers. After feature extraction, the classification phase follows. Feature maps are flattened into a 1D vector, serving as input for the first Fully Connected (FC) layer. The output of this layer goes to the second FC layer, which is a softmax classifier. The dataset and the implementation source code are available as open source [30]. The LTE and NR samples were collected from the LTE and NR network simulators. For the Overlap class, samples were collected by merging the LTE and NR signals with a randomly changing offset. A TRW size of 44 μs [25] and a sampling rate of 20 Msps were used for the data collection. Hence, each example signal has 880 IQ samples. To cover various channel conditions, SNR levels of -15 to 30 dB were considered (at a step of 5 dB). For each class, 7500 examples were collected at each considered SNR level. The FFT of the IQ samples was then used as input to train and validate a CNN-based TR model that could distinguish between the three classes of signals. 70% of the total dataset was randomly selected for training, while the remaining 30% was used for validation and testing the CNN model. The classification performance of the CNN model at different SNR levels is shown in Fig. 4. It can be observed that the CNN model has a classification accuracy surpassing 98% for SNRs of 5 dB or higher.

Additionally, a traffic pattern characterization scheme is proposed for estimating the pattern of the muted LTE MBSFN subframes and the muted NR MBS subframes that can be utilized by the NR and LTE schedulers. The technology recognition model is used to identify the type of signal present in each TRW. During the traffic pattern characterization procedure, consecutive TRWs that have been identified as belonging to the same technology are added to determine the signal type in each subframe. As the proposed DSS algorithms use the detection of collisions to initiate a new pattern sensing window, misclassification of an Overlap class can trigger a new pattern sensing window. In the pattern sensing window, the cross-band traffic offloading is stopped until the new pattern is estimated. Hence, frequent pattern-sensing windows triggered by misclassified overlap windows can lead to poor spectrum utilization. To minimize this, the detection of two consecutive overlap TRWs is used to indicate the occurrence of a collision and trigger spectrum sensing.

In the proposed DSS schemes, resource allocation decisions are made based on the outcome of the TRTC system. Hence, an optimal batch size has to be selected in such a way that the TRTC reports the traffic pattern in the shortest possible duration. Fig. 5a shows the processing time required for the pre-processing stage, the CNN model execution, and the overall process for different batch sizes. The figure shows that the processing time keeps increasing as the batch size increases. The benchmarks were executed on a host machine equipped with an AMD Ryzen 9 5900X 12-Core Processor, an NVIDIA RTX 3090 GPU, and 64GB of RAM. Fig. 5b shows the classification rate in every subframe (1 ms). For the 44 μs TRW, 1 ms duration is composed of approximately 23 TRWs. This means that a minimum of 23 TRWs have to be classified within 1 ms duration. The figure shows that a batch size of at least 16 TRWs is required to achieve the 23 TRWs/ms target classification rate.

Fig. 5c shows the probability of collision (overlap class) for different batch sizes. The probability of collision is determined from the statistics of identified TRWs collected throughout the simulation duration for different batch sizes. The lowest collision probability is obtained when a 16-TRW batch size is used. For batch sizes greater than 16 TRWs, the processing time delay keeps increasing, and this increases the probability of collision as there is a higher delay before a new resource allocation is used based on the outcome of the TRTC system. Similarly, for batch sizes smaller than 16 TRWs, the classification rate drops below the required 23 TRWs/ms leading to a delay before a new resource allocation is used based on the outcome of the TRTC system for the TRWs in 1 ms. This delay in a new resource allocation leads to an increased probability of collisions. Based on these results, a batch size of 16 TRWs is used for the TRTC system employed in the proposed DSS solution.

C. Performance of LTE Scheduler in LTE band

Fig. 6a shows the CDF of the obtained LTE throughput for the LTE network using the PF LTE scheduler and the customized PF LTE scheduler. Below the median of the CDF, it can be observed that the LTE throughput obtained using the proposed customized PF LTE scheduler is lower than the LTE throughput obtained using the PF LTE scheduler. For example, the probability of getting LTE throughput below 30 Mbps is 32% and 36% for the PF LTE scheduler and the proposed customized PF LTE scheduler, respectively. This happens due

to the fact that the customized PF LTE scheduler checks the traffic load of the active UEs and updates its scheduling every 160 TTIs (Algorithm 1). If the traffic demand increases within the 160 TTI window, the obtained throughput is limited to the maximum capacity of the resources defined based on the traffic load at the beginning of the scheduling window. If the traffic load is closer or higher than the system capacity of the LTE band, the customized PF LTE scheduler uses all the PRBs of the LTE band, as in the case of the PF LTE scheduler. Hence, the throughput CDFs are close for the higher throughput values.

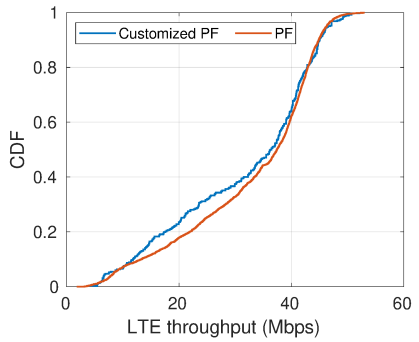

(a)

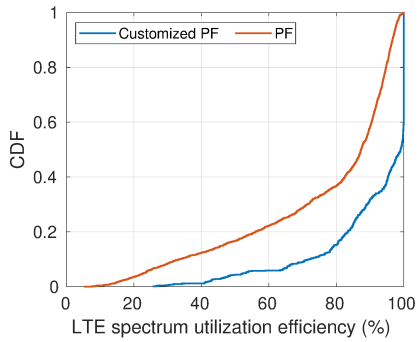

(b)

Fig. 6: Performance of the PF LTE scheduler and the customized PF LTE scheduler in the LTE band: a) CDF of LTE throughput; b) CDF of LTE spectrum utilization efficiency.

The CDF of LTE spectrum utilization efficiency for the PF LTE scheduler and customized PF LTE schedulers is given in Fig. 6b. The spectrum utilization efficiency (ξ_s) of the schedulers in the simulation is computed in every scheduling window as follows:

$$\xi_s = \frac{U_{rb}}{A_{rb}} * 100\%. \tag{28}$$

where U_{rb} is the number of PRBs actually allocated to active UEs (based on the traffic) and A_{rb} is the total number of available PRBs in the resource pool of the scheduler. For the PF LTE scheduler, all PRBs within the LTE band are available in the resource pool of the scheduler. On the other hand, the resource pool of the customized PF LTE scheduler is adaptively configured to include resources in certain TTIs only, while the rest of the TTIs are part of the resource pool as they are assigned to muted MBSFN subframes.

At the median of the CDF (Fig. 6b), a spectrum utilization efficiency of 87% and 99% is obtained for the PF LTE scheduler and the proposed customized PF LTE scheduler, respectively, showing that the customized PF LTE scheduler has higher spectrum utilization efficiency as the PRBs available for the scheduler are adjusted based on the traffic.

D. Performance of NR Scheduler in NR band

The CDF plots of the obtained NR throughput with the PF NR scheduler and the customized PF NR scheduler are depicted in Fig. 7a. The NR throughput obtained with the proposed customized NR scheduler is slightly lower than the NR throughput obtained with the PF NR scheduler. As an example, the likelihood of achieving an NR throughput of less than 60 Mbps is 69% for the PF NR scheduler and 72% for the customized PF NR scheduler. The customized PF NR scheduler checks the traffic load of the active UEs and updates its scheduling every 80 TTIs (Algorithm 3). In the event that traffic demand rises during this window, the obtained throughput will be capped at the maximum capacity of the resources, as determined by the traffic load at the start of the scheduling window. However, the gap between the throughput CDF curves of the PF NR scheduler and customized PF NR scheduler (Fig. 7a) is very low, and it is lower than the gap between the throughput CDF curves of the PF LTE scheduler and customized PF LTE scheduler Fig. 6a. This can be explained by the fact that the customized PF NR scheduler updates its resource pool in 80 ms, which is shorter than the 160 ms period required to update the resource pool of the customized PF LTE scheduler.

Fig. 7b shows the CDF of the efficiency with which the PF LTE scheduler and customized PF NR scheduler use the corresponding available resource pools in the NR band. The results show that the customized PF NR scheduler has a higher spectrum utilization efficiency as compared to the PF NR scheduler. Similar to the LTE spectrum utilization efficiency, the NR spectrum utilization efficiency is computed using eq. 28. In the PF NR scheduler, all PRBs within the NR band are available in the resource pool of the scheduler, which leads to poor spectrum utilization efficiency. To counter this, the proposed NR resource controller determines the size of the resource pool of the customized PF scheduler based on the traffic load, and the remaining resources within the muted MBS subframes are not part of the resource pool of the scheduler.

The shorter resource pool update period used by the customized PF NR scheduler and its higher flexibility to allocate muted MBS subframes lead to higher spectrum utilization efficiency gains as compared to the PF NR scheduler. As an example, the likelihood of getting less than 80% spectrum utilization efficiency is 40% and 9% for the PF scheduler and the customized PF NR scheduler, respectively.

E. LTE and NR Performance using Cross-band DSS

In this section, we present the performance of the LTE and NR networks considering cross-band DSS. Fig. 8c shows the spectrogram of LTE and NR signals from the simulator on

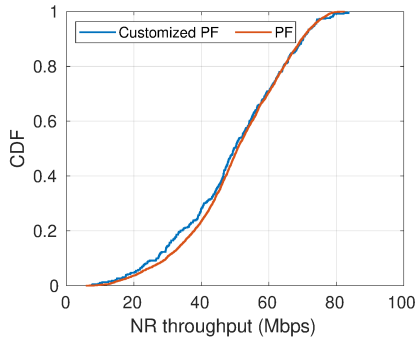

(a)

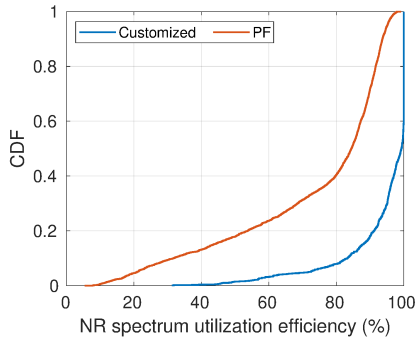

(b)

Fig. 7: Performance of the PF NR scheduler and the proposed customized PF NR scheduler in the NR band: a) CDF of NR throughput; b) CDF of NR spectrum utilization efficiency.

a randomly selected sample frame on the LTE band. Based on the LTE traffic at the shown sample frame, the LTE resource controller limits the resource pool of the customized PF LTE scheduler to utilize resources in the four subframes only, leaving the six remaining subframes as muted MBSFN subframes (Fig. 8a). The figure shows that the non-MBSFN region of the muted MBSFN subframes is reserved for the always-on LTE control signals. The NR resource controller, on the other hand, senses the LTE band and determines the pattern of the muted MBSFN subframes. The resources in these muted MBSFN subframes are used by the NR scheduler (Fig. 8b).

Fig. 9 shows the CDF for LTE and NR throughput obtained with and without cross-band DSS. The figure shows the CDF (over all the simulation duration) of throughput obtained for an LTE network with a static LTE band, an NR network with a static NR band, an LTE network with TRTC-based uncoordinated cross-band DSS, an NR network with TRTC-based uncoordinated cross-band DSS, an LTE network with signaling channel-based coordinated cross-band DSS, and an NR network with signaling channel-based coordinated cross-band DSS. The results are obtained by using the proposed customized PF scheduler for both technologies. Without the use of the DSS, the customized PF LTE scheduler and customized PF NR scheduler have resource pools limited to the resources in the static LTE and NR bands, respectively. For this reason, the results show that there is an LTE and NR throughput gain using cross-band DSS as compared to the corresponding throughput obtained using a static band.

For the LTE network, the maximum obtained throughput is 53.2 Mbps and 81.4 Mbps using the static LTE band and cross-band DSS, respectively. As the number of active UEs varies in a Poisson distribution between 1 and 100, with a mean of 50, the probability that the LTE band is at its maximum capacity is high. Based on the results, the highest capacity of the static LTE band-based LTE network ranges between 37.4 Mbps and 53.2 Mbps, depending on the location of the UEs and channel conditions. For this reason, the throughput probability distribution is high in this range for the LTE network designed to utilize the static LTE band only. On the other hand, the LTE network that utilizes cross-band DSS has a throughput distribution that reaches up to 81.4 Mbps. As the NR network mainly utilizes the NR band, it is less probable to get a completely free NR band that is available to offload the LTE traffic. Hence, the probability of getting throughput values close to the maximum value is low.

For the NR networks considered with a static NR band and with cross-band DSS, the maximum throughput obtained is 80.1 Mbps and 105.3 Mbps, respectively. Likewise, in the case of an LTE network with a static LTE band, there is a significant possibility that the NR band is at maximum capacity as the number of active NR UEs varies from 1 to 100 according to a Poisson distribution, with a mean of 50. Depending on the distribution of UEs and the channel conditions, the results show that the maximum capacity of a static band-based NR network can be anywhere from 60.8 Mbps to 80.1 Mbps. By contrast, the cross-band DSS-based NR network can deliver a throughput of up to 105.3 Mbps. The CDF shows a slowly increasing trend as the throughput approaches its upper bound. The reason for this is that the LTE network predominately utilizes the LTE band, making it less probable that a completely free LTE band will be available to offload the NR traffic. Taking into account the entire simulation time, the introduction of the TRTC-based uncoordinated cross-band DSS improves the average throughput of LTE and NR bands by 13.5% and 8.3%, respectively.

Additionally, the Fig. 9 illustrates that by eliminating the need for a coordination channel and implementing a TRTC-based cross-band DSS scheme, there is a marginal drop in the achieved LTE and NR throughput as compared to the coordinated cross-band DSS approach. For the coordinated cross-band DSS, we consider that the eNB uses Algorithm 1 to schedule muted MBSFN subframes on the LTE band and the gNB uses Algorithm 2 to schedule muted MBS subframes on the NR band. Based on the minimum possible periodicity of the resource pool management scheme, the eNB uses a dedicated coordination channel to send scheduling updates to the gNB every 160 ms, and the NR scheduler uses the available resources on the LTE band based on the received scheduling information. Similarly, the gNB sends scheduling updates to the eNB every 80 ms via a coordination channel, and the LTE scheduler uses the available resources on the NR band based on the received scheduling information. In comparison to the coordinated cross-band DSS approach, the TRTC-based cross-band DSS scheme results in a reduction of 3.1% and 2.3% in the attained average LTE and NR throughput, respectively. The marginal drop occurs due to reactive resource management

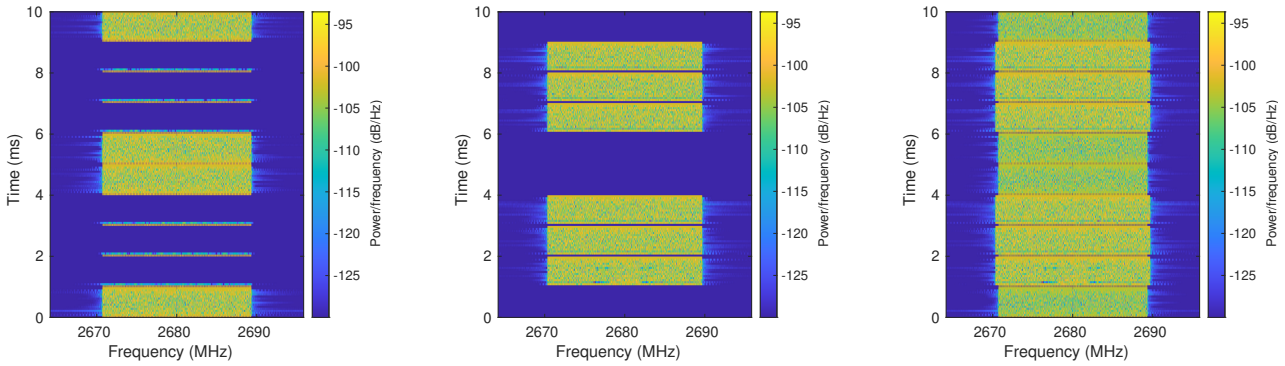

(a) LTE (b) NR (c) LTE and NR

Fig. 8: Spectrogram of LTE, NR, and combined (using proposed cross-band DSS) signals in a sample frame in the LTE band.

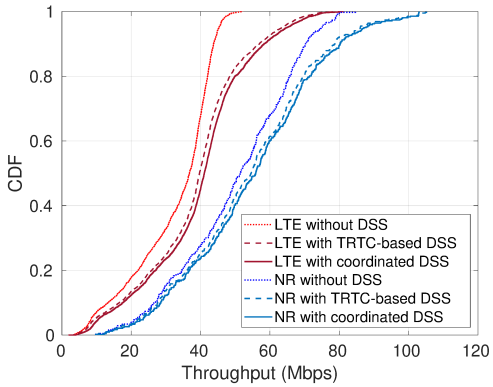

Fig. 9: LTE and NR throughput using static bands, using TRTC-based cross-band DSS, and using coordinated cross-band DSS.

when an overlapping transmission or unused subframes occur in the TRTC-based cross-band DSS, while the coordinated cross-band DSS uses proactive resource management based on the scheduling information exchanged through the dedicated signaling channel.

The CDF of the spectrum utilization efficiency of LTE and NR bands considering LTE and NR networks with and without DSS is shown in Fig. 10. The figure shows the CDF of spectrum utilization efficiency for the LTE and NR bands using static configuration, TRTC-based uncoordinated cross-band DSS, and signaling channel-based coordinated cross-band DSS. In the simulation, the spectrum utilization efficiency on a specific band (ξ_b) is periodically determined using the following formula:

$$\xi_b = \frac{U_{rb}}{T_{rb}} * 100\%. \tag{29}$$

where U_{rb} is the number of PRBs allocated to active UEs and T_{rb} is the total number of available PRBs in the band. Without the use of DSS, PRBs are allocated to LTE and NR UEs in the LTE and NR bands, respectively. On the other hand, the PRBs in each band can be allocated to LTE and NR UEs when the proposed cross-band DSS scheme is proposed.

Fig. 10 shows that the spectrum utilization efficiency is enhanced with the help of DSS in both LTE and NR bands. With the introduction of the proposed DSS scheme, the spectrum utilization efficiency gain achieved in the NR band is higher than the spectrum utilization efficiency gain obtained in the LTE band. As an example, the likelihood of getting less than 60% spectrum utilization efficiency is 23.2%, 23.6%, 10.6%, and 3.4% for LTE bands without DSS, NR bands without DSS, LTE bands with TRTC-based DSS, and NR bands with TRTC-based DSS, respectively. The reason for getting higher spectrum utilization efficiency on the NR band (with TRTC-based DSS) is the fact that the NR band is primarily used by the NR network, which has a shorter resource pool update period (80 ms) and higher flexibility to allocate muted MBS subframes as compared to the LTE network, which can allocate a maximum of six muted MBSFN subframes with a longer resource pool update period (160 ms).

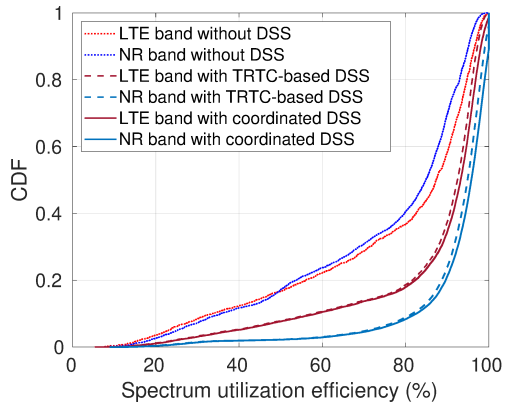

Fig. 10: Spectrum utilization efficiency of LTE and NR bands without DSS, with TRTC-based cross-band DSS, and coordinated cross-band DSS.

Considering the overall simulation duration, the introduction of TRTC-based DSS gives 11.8% and 20.7% improvements in the spectrum utilization efficiency of LTE and NR bands, respectively. Fig. 10 also shows that the TRTC-based DSS scheme and the coordinated DSS approach have comparable

performance with respect to spectrum utilization efficiency. As compared to the coordinated DSS, the TRTC-based DSS has a drop of less than 2% in spectrum utilization efficiency in the LTE and NR bands. This minor drop is attributed to the presence of unused subframes during the monitoring phases of the radio resource management schemes by the LTE and NR schedulers.

We have also evaluated the performance of the proposed DSS scheme in terms of the probability of buffer overflow. A buffer overflow occurs when the data buffer becomes full and new data arrives. When this happens, the buffer cannot accommodate any more data, and packets are dropped. We used a buffer size of 50,000 bits [31] for each UE, and the total number of times the traffic queue exceeds this value is counted to measure the average buffer overflow probability. The results show that the probability of buffer overflow is 14.6%, while it drops to 9.4% and 9.1% when the TRTC-based DSS and coordinated DSS are used, respectively.

VI. Conclusions and Future Work

In this work, we present a cross-band DSS scheme utilizing the MBSFN feature of an LTE network and the MBS feature of an NR network. To enable the proposed cross-band DSS scheme, novel uncoordinated LTE and NR resource controllers are proposed. Based on traffic requirements in the LTE band, the LTE resource controller dynamically assigns muted MBSFN subframes that the NR scheduler can use. Similar to this, the LTE scheduler can take advantage of muted MBS subframes in the NR band. The proposed DSS technique differs from the state-of-the-art in that it does not require a coordination signaling channel between the LTE and NR networks. A TRTC system is utilized to recognize and characterize the traffic pattern of the co-located cells instead of a resource coordination channel. Based on the results of the TRTC, the LTE scheduler offloads its traffic into the NR band and vice versa. The proposed cross-band DSS improves the average LTE throughput, average NR throughput, average LTE band spectrum utilization efficiency, and average NR band spectrum utilization efficiency by 13.5%, 8.3%, 11.8%, and 20.7%, respectively.

In this work, we assumed subframe-level synchronization between the LTE eNB and NR gNB and developed our solution based on that. Nonetheless, the exploration and assessment of the synchronization mechanisms could be considered a potential future work. Additionally, the proposed DSS scheme uses the TRTC system, which assesses the existing traffic load and makes the subsequent resource allocation decision. This resource allocation decision can be extended so that the decisions are executed proactively by integrating advanced machine learning-based traffic prediction techniques.

References

[1] M. Shafi, A. F. Molisch, P. J. Smith, T. Haustein, P. Zhu, P. De Silva, F. Tufvesson, A. Benjebbour, and G. Wunder, "5G: A Tutorial Overview of Standards, Trials, Challenges, Deployment, and Practice," IEEE Journal on Selected Areas in Communications, vol. 35, pp. 1201–1221, June 2017.

[2] "TS 38.101-4, 5G; NR; User Equipment (UE) radio transmission and reception; Part 4: Performance requirements," tech. rep., 3GPP Release 17, 2022.

[3] J. G. Andrews, S. Buzzi, W. Choi, S. V. Hanly, A. Lozano, A. C. K. Soong, and J. C. Zhang, "What Will 5G Be?," IEEE Journal on Selected Areas in Communications, vol. 32, pp. 1065–1082, June 2014.

[4] M. Sergey, Y. Chung-Cheng, and A. E.-s. Mohamed, "5G NR and 4G LTE Coexistence: A Comprehensive Deployment Guide to Dynamic Spectrum Sharing, MEDIATEK White Paper," tech. rep., 2020.

[5] V. K. Shrivastava, S. Baek, and Y. Baek, "5G Evolution for Multicast and Broadcast Services in 3GPP Release 17," IEEE Communications Standards Magazine, vol. 6, no. 3, pp. 70–76, 2022.

[6] "TS 23.246, V14.1.0 Multimedia Broadcast/Multicast Service (MBMS), Architecture and functional description," tech. rep., 3GPP, Release 14, May 2017.

[7] Samsung, "Dynamic Spectrum Sharing, Technical White Paper," tech. rep., 2021.

[8] B. Cai, X. Zhao, C. Hu, and W. Xie, "Analysis of spectrum refarming methods for 5g network deployment," in 2022 International Conference on Information Processing and Network Provisioning (ICIPNP), pp. 52–56, 2022.

[9] "TS 38.331 , Introduction of a New NR Band for LTE/NR Spectrum Sharing in Band 41/n41," tech. rep., 3GPP Release 15, 2019.

[10] "TS 38.331 , Introduction of Enhanced Support for Dynamic Spectrum Sharing," tech. rep., 3GPP Release 16, 2019.

[11] M. Wei, X. Li, W. Xie, and C. Hu, "Practical Performance Analysis of Interference in DSS System," Applied Sciences, vol. 13, no. 3, 2023.

[12] J. Xin, S. Xu, H. Zhang, and S. Xiong, "Efficient Dynamic Spectrum Sharing for LTE-NR Networks," in Proceedings of the 2021 2nd International Conference on Electronics, Communications and Information Technology (CECIT), pp. 538–543, 2021.

[13] J. Xin, S. Xu, and L. Zhang, "Dynamic Spectrum Sharing for NR-LTE Networks," in 2021 2nd Information Communication Technologies Conference (ICTC), pp. 161–164, 2021.

[14] G. Barb, M. Otesteanu, and M. Roman, "Dynamic Spectrum Sharing for LTE-NR Downlink MIMO Systems," in Proceedings of the 2020 International Symposium on Electronics and Telecommunications (ISETC), pp. 1–4, 2020.

[15] U. Challita and D. Sandberg, "Deep Reinforcement Learning for Dynamic Spectrum Sharing of LTE and NR," in Proceedings of the ICC 2021 - IEEE International Conference on Communications, pp. 1–6, 2021.

[16] G. Barb, F. Alexa, and M. Otesteanu, "Dynamic Spectrum Sharing for Future LTE-NR Networks," Sensors, vol. 21, no. 12, 2021.

[17] S. Kim, "4G/5G Coexistent Dynamic Spectrum Sharing Scheme based on Dual Bargaining Game Approach," Computer Communications, vol. 181, pp. 215–223, 2022.

[18] M. Pini, A. Minetto, A. Vesco, D. Berbecaru, L. M. C. Murillo, P. Nemry, I. De Francesca, B. Rat, and K. Callewaert, "Satellite-derived Time for Enhanced Telecom Networks Synchronization: the ROOT Project," in Proceedings of the 2021 IEEE 8th International Workshop on Metrology for AeroSpace (MetroAeroSpace), pp. 288–293, 2021.

[19] "TR 26.849, Technical Specification Group Services and System Aspects; Multimedia Broadcast/Multicast Service MBMS improvements; MBMS operation on demand," tech. rep., 3GPP Release 12, 2015.

[20] "TS 36.213, LTE; Evolved Universal Terrestrial Radio Access (E-UTRA),Physical Layer Procedures," tech. rep., 3GPP, Release 17, 2022.

[21] "TS 38.214, NR; Technical Specification Group Radio Access Network, Physical Layer Procedures for Data," tech. rep., Release 17, 2022.

[22] "TS 138.331, 5G NR; Protocol Specification, Radio Resource Control (RRC) ," tech. rep., 3GPP TS Release 17, 2022.

[23] "TR 38.912, Technical Specification Group Radio Access Network; Study on New Radio (NR) access technology," tech. rep., 3GPP Release 17, 2022.

[24] M. Maman, E. Catte, M. Sana, M. Girmay, V. Maglogiannis, D. Naudts, H. Lee, F. Carrez, A. Anttonen, Y. Fernandez, J. Moreno, V. Lamprousi, and V. Stavroulaki, "Coverage Extension as a Service for Flexible 6G Networks Infrastructure," in Proceedings of the 2022 IEEE Globecom Workshops (GC Wkshps), pp. 1329–1334, 2022.

[25] M. Girmay, V. Maglogiannis, D. Naudts, M. Aslam, A. Shahid, and I. Moerman, "Technology Recognition and Traffic Characterization for Wireless Technologies in ITS Band," Vehicular Communications, vol. 39, p. 100563, 2023.

[26] I. Khalid, M. Girmay, V. Maglogiannis, D. Naudts, A. Shahid, and I. Moerman, "An Adaptive MBSFN Resource Allocation Algorithm for Multicast and Unicast Traffic," in Proceedings of the 2023 IEEE 20th

Consumer Communications Networking Conference (CCNC), pp. 579–586, 2023.
[27] The vienna lte-advanced simulators. New York, NY: Springer Berlin Heidelberg, 2016.
[28] "Traffic Models for IEEE 802.20 MBWA System Simulations," IEEE Working Group 802.20 Permanent Document, 2003.
[29] M. Girmay, V. Maglogiannis, D. Naudts, A. Shahid, and I. Moerman, "Coexistence Scheme for Uncoordinated LTE and WiFi Networks Using Experience Replay Based Q-Learning," Sensors, vol. 21, no. 21, 2021.
[30] M. Girmay, "Dataset for FFT of IQ samples: LTE, NR, and Overlap ," 2023. https://dx.doi.org/10.21227/6bj3-7720.
[31] R. Zhu and J. Yang, "Buffer-aware Adaptive Resource Allocation Scheme in LTE Transmission Systems," EURASIP Journal on Wireless Communications and Networking, vol. 2015, no. 1, 2015.

Merkebu Girmay received his M.Sc. degree in Communication Engineering from Mekelle University, Tigray, in 2014. After his studies, he worked as an academic staff in Mekelle University until he joined IDLab, University of Ghent–imec, Belgium in December 2018. His main research interests include radio network resource management and optimization, software-defined radios, spectrum sharing, V2X communications, IEEE802.11, 4G LTE, 5G NR, and 6G networks.

Vasilis Maglogiannis received his M.Eng degree in Computer Engineering and his M.Sc in Science and Technology of Computers, Telecommunications and Networks from University of Thessaly, Greece in 2012 and 2014 respectively. In 2018, he received his Ph.D degree in Computer Science Engineering from the Department of Information Technology of Ghent University. From 2019 to 2021, he worked as a Postdoctoral Researcher at IDLab, Univeristy of Ghent in collaboration with imec, Belgium. Since 2021, he is affiliated with imec. His main research interests include mobile and wireless networks, 5G/6G networks, 802.11, Cooperative Intelligent Transport Systems (C-ITS).

Dries Naudts received the Master's degree in Computer Science from the Ghent University, Belgium in 2001. After his studies, he started as a software engineer in industry. In April 2005, he joined the imec IDLab Research Group, where he is currently active as a senior researcher. His main research interest is in mobile wireless networks, 4G, 5G, C-ITS, V2X, IEEE 802.11, ad hoc and mesh networking, IPv6, wireless testbeds. He is working on several national and European projects in close collaboration with other academic and industrial partners.

Timo De Waele received his M. Sc in Computer Science in 2020 from Ghent University, Belgium. After his graduation he started working as a PhD student at the iWINE-UGent/IDLab/imec research group. In 2021 he became a PhD fellow of the FWO-V (Research Foundation - Flanders). His scientific work mainly focuses on developing unsupervised and semi-supervised machine learning algorithms using data from biosignals such as electrocardiograms and movement data from accelerometers and gyroscopes.

Prof. dr. ir. Eli De Poorter is professor at the IDLab research group from Ghent University and imec (https://idlab.technology). He received his master degree in Computer Science Engineering from Ghent University, Belgium, in 2006, his Ph.D. degree in 2011 and he became professor at IDLab in 2015. His team performs research on wireless communication technologies such as (indoor) localization solutions, wireless IoT solutions and machine learning for wireless systems.

Adnan Shahid (M'15 - SM'17) received the B.Sc. and M.Sc. degrees in computer engineering from the University of Engineering and Technology, Taxila, Pakistan, in 2006 and 2010, respectively, and the Ph.D. degree in information and communication engineering from Sejong University, South Korea, in 2015. He is Professor in the Internet Technology and Data Science Lab (IDLab) of Ghent University and imec. His research interests include machine learning and artificial intelligence for wireless communications and networks, decentralized learning, radio resource management, the Internet of Things, 5G/6G networks, localization, connected healthcare, etc.

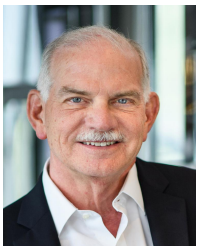

H. Vincent Poor (S'72, M'77, SM'82, F'87) received the Ph.D. degree in EECS from Princeton University in 1977. From 1977 until 1990, he was on the faculty of the University of Illinois at Urbana-Champaign. Since 1990 he has been on the faculty at Princeton, where he is currently the Michael Henry Strater University Professor. During 2006 to 2016, he served as the dean of Princeton's School of Engineering and Applied Science. He has also held visiting appointments at several other universities, including most recently at Berkeley and Cambridge. His research interests are in the areas of information theory, machine learning and network science, and their applications in wireless networks, energy systems and related fields. Among his publications in these areas is the recent book *Machine Learning and Wireless Communications*. (Cambridge University Press, 2022). Dr. Poor is a member of the National Academy of Engineering and the National Academy of Sciences and is a foreign member of the Chinese Academy of Sciences, the Royal Society, and other national and international academies. He received the IEEE Alexander Graham Bell Medal in 2017.

Ingrid Moerman (Senior Member, IEEE) received her degree in Electrical Engineering (1987) and the Ph.D. degree (1992) from the Ghent University, where she became a part-time professor in 2000. She currently combines a full professor position with part-time allocation at Ghent University and is a staff member at IDLab, a core research group of imec with research activities embedded in Ghent University and University of Antwerp. Dr. Moerman is program manager of the 'Deterministic Networking' track, part of the connectivity program at imec, and in this role she coordinates research activities on end-to-end wired/wireless networking solutions driven by professional and mission-critical applications that have to meet strict Quality of Service requirements in terms of throughput, bounded latency and reliability in challenging application areas like industrial automation, vehicular networks, safety-critical operations, professional entertainment, etc. Ingrid Moerman has a longstanding experience in running and coordinating national and EU research funded projects.